Spectral sensitivity in Onychophora (velvet worms) revealed by electroretinograms, phototactic behaviour and opsin gene expression

Holger Beckmann[1,2]*, Lars Hering[1], Miriam J. Henze[3], Almut Kelber[3], Paul A. Stevenson[4] and Georg Mayer[1]

[1]Animal Evolution and Development, Institute of Biology, University of Leipzig, Talstrasse 33, D-04103 Leipzig, Germany
[2]Rudolf-Boehm-Institute of Pharmacology and Toxicology, University of Leipzig, Haertelstrasse 16-18, D-04107 Leipzig, Germany
[3]Department of Biology, Lund University, Sölvegatan 35, 22362, Lund, Sweden
[4]Animal Physiology, Institute of Biology, University of Leipzig, Talstraße 33, D-04103 Leipzig, Germany

*Author for correspondence: Rudolf-Boehm-Institute of Pharmacology and Toxicology, University of Leipzig, Haertelstrasse 16-18, D-04107 Leipzig, Germany (holger.beckmann@medizin.uni-leipzig.de)

Manuscript type: Research article

Short title: Spectral Sensitivity in Onychophora

ABSTRACT

Onychophorans typically possess a pair of simple eyes, inherited from the last common ancestor of Panarthropoda (Onychophora + Tardigrada + Arthropoda). These visual organs are thought to be homologous to the arthropod median ocelli, whereas the compound eyes most likely evolved in the arthropod lineage. To gain insights into the ancestral function and evolution of the visual system in panarthropods, we investigated phototactic behaviour, opsin gene expression and the spectral sensitivity of the eyes in two representative species of Onychophora: *Euperipatoides rowelli* (Peripatopsidae), and *Principapillatus hitoyensis* (Peripatidae). Our behavioural analyses, in conjunction with previous data, demonstrate that both species exhibit photonegative responses to wavelengths ranging from ultraviolet to green light (370–530 nm), while electroretinograms reveal that the onychophoran eye is maximally sensitive to blue light (peak sensitivity ~480 nm). Template fits to the obtained sensitivities suggest that the onychophoran eye is monochromatic. To clarify on which type of opsin the single visual pigment is based, we localised the corresponding mRNA in the onychophoran eye and brain using *in situ* hybridization. Our data show that the *r-opsin* gene (*onychopsin*) is expressed exclusively in the photoreceptor cells of the eye, whereas the *c-opsin* mRNA is confined to optic ganglion cells and the brain. Together, our findings suggest that the onychopsin is involved in vision, whereas the c-opsin might have a photoreceptive, non-visual function in onychophorans.

KEY WORDS: Arthropod, Eye, Light response, Vision, Opsins, Phototaxis, Evolution

INTRODUCTION

Onychophorans (velvet worms) typically bear a pair of simple, ocellus-like eyes (Fig. 1A,B), which are thought to be homologous with the median ocelli of arthropods (Mayer, 2006), one of their closest relatives (Giribet and Edgecombe, 2012). Accordingly, the last common ancestor of Panarthropoda (Onychophora + Tardigrada + Arthropoda) most likely possessed a pair of ocellus-like visual organs, whereas the compound eyes evolved within the arthropod lineage (Mayer, 2006; Hering et al., 2012; Hering and Mayer, 2014). While all arthropod species studied thus far have multiple rhabdomeric opsins (r-opsins) as visual pigments, their presence being a prerequisite for colour vision (reviewed by Briscoe and Chittka, 2001), transcriptomic analyses of the opsin repertoire revealed only one r-opsin gene (*onychopsin*) in five distantly related onychophoran species (Hering et al., 2012). In phylogenetic analyses, *onychopsin* forms the sister group to the visual r-opsins of arthropods, suggesting that this gene functions in onychophoran vision. However, a ciliary-type opsin (c-opsin, to which type also the visual pigments of vertebrates belong; reviewed by Porter et al., 2012), has also been reported to occur in the onychophoran eye (Eriksson et al., 2013). Hence, a detailed expression study at the cellular level seems necessary to clarify whether r- or c-type opsins, or both, are involved in onychophoran vision.

Behavioural studies revealed negative phototactic behaviour in two species of Peripatidae: *Epiperipatus biolleyi* (see Monge-Nájera et al., 1993), and *Principapillatus hitoyensis* (referred to as "*Epiperipatus* cf. *isthmicola*" in Hering et al., 2012). Specimens of *P. hitoyensis* showed a photonegative reaction to wavelengths ranging from 363 nm (ultraviolet, UV) to 586 nm (yellow). The sensitivity maximum (α-peak) of the visual pigment in this species was therefore estimated to be in the blue-green range of the spectrum (Hering et al., 2012). However, neither the specific wavelength of the α-peak nor the actual spectral sensitivity curve of the onychophoran photoreceptors is known. Moreover, it is unclear whether a photonegative reaction to the same wavelengths occurs in representatives of the second major onychophoran subgroup, the Peripatopsidae, for which quantitative data are still missing.

We therefore analysed the behavioural response to light and localised the expression of the r- and c-type opsins in the peripatopsid *Euperipatoides rowelli*. To identify the sensitivity maximum (α-peak) of the visual pigment and to complement

previous data from *P. hitoyensis*, we additionally performed electrophysiological recordings from the eye in both *E. rowelli* and *P. hitoyensis*. The obtained data allow conclusions regarding the physiological properties and function of the visual system in the last common ancestor of Onychophora and Panarthropoda, respectively.

RESULTS

Spectral sensitivity of the onychophoran eye

We recorded electroretinograms (ERGs), extracellular, light-induced potential changes in the retina, from the eyes of six specimens of *E. rowelli* of both sexes and one male of *P. hitoyensis* (Fig. 2A,B). Responses to light flashes of 40 or 100 ms duration consisted of an initial hyperpolarization truncated by a depolarization (Fig. 3A,C). The half width of the response (width at half maximal hyperpolarization) exceeded 140 ms and the time to peak (time interval from stimulus onset to maximal hyperpolarization) exceeded 95 ms for all tested intensities. Both values increased considerably with decreasing stimulus intensity (Fig. 3A,C). Spectral flashes with equal photon flux revealed that the dark-adapted retina was most sensitive to wavelengths around 480 nm, i.e. to the region of the spectrum perceived as blue by humans. We fitted template formulae (Govardovskii et al., 2000), which approximate the absorbance spectra of opsin-based visual pigments in invertebrates (Stavenga, 2010), to the data from each individual (Fig. 3B,D) and averaged the results for different individuals of the same species. Optimal fits were obtained assuming a visual pigment with an absorbance peak at 474 ± 6.5 nm (wavelength λ_{max}: average ± standard deviation; coefficient of determination: $R^2 = 0.88 \pm 0.03$) for the six specimens of *E. rowelli* and at 484 nm ($R^2 = 0.93$) for one specimen of *P. hitoyensis*. When the eye was adapted to green light, responses were indistinguishable from noise level, and no other sensitivity peaks were apparent at shorter wavelengths. During recovery from green adaptation, the shape of the spectral curve continued to be similar to the curve of the dark-adapted retina (supplementary material Fig. S1).

Localisation of the r- and c-type opsins in the onychophoran eye and brain

To determine whether the signal obtained from the electrophysiological recordings is related to the onychophoran r- or c-type opsin, we performed fluorescence *in situ*

hybridization experiments on cryosections of the *E. rowelli* heads (Fig. 4A–F). Our data show that *Er-onychopsin* is expressed in the photoreceptor layer of each eye, and lacking in other tissues, including the brain (N=6; Fig. 4B–D; supplementary material Fig. S2). In contrast, *Er-c-opsin* mRNA is localised both in optic ganglion cells within the eye and in numerous neuronal somata within the brain, in particular in the ventral perikaryal layer of the protocerebrum (Fig. 4E,F; supplementary material Fig. S2). A few additional *Er-c-opsin* expressing cells are seen in the deutocerebrum and in the medullary cords (=connecting cords) linking the brain to the ventral nerve cords (Fig. 4E,F). Most importantly, and in contrast to optic ganglion cells, *Er-c-opsin* mRNA is not expressed in the photoreceptor layer of the eye (Fig. 4E).

Our control experiments using the sense probe for *Er-onychopsin* revealed no signal within the eye, indicating that the obtained labelling using the antisense probe for *Er-onychopsin* is specific (supplementary material Fig. S2). The unspecific labelling in the cuticle lining the epidermis and pharyngeal lumen, which occurs in all our preparations, is due to autofluorescence. In contrast, applying the *Er-c-opsin* sense probe revealed a similar pattern to the *Er-c-opsin* antisense probe (supplementary material Fig. S2). The same result was obtained repeatedly in all experiments using different sense probes on cryosections of different individuals (N=4), whereas an increase of the hybridization temperature to 58 °C completely abolished the labelling in all reactions, irrespective of whether the sense or antisense probes were used.

Behavioural response of onychophorans to light of different wavelengths

To clarify whether *E. rowelli* shows negative phototaxis, single animals were released in a dark arena and left free to move in any direction. On directing a bright white light at their heads, the animals immediately changed walking direction away from the light source (Fig. 5A; Wilcoxon-signed-rank test: $p<0.001$), but did not veer from course in control experiments without the light stimulus (Fig. 5B).

To determine the sensitivity threshold of *E. rowelli*'s negative phototaxis, we used a blue light-emitting diode (λ_{max} = 465 nm, i.e., close to the sensitivity maximum obtained from the electroretinograms, cf. Fig. 3B). Up to 6 animals were grouped (N=7 groups) and released simultaneously in one half of a dark arena, after which this half was illuminated with blue light of four different intensities (3×10^{11}, 6×10^{11}, 9×10^{11},

12×10^{11} photons cm^{-2} s^{-1}, measured at the bottom of the arena) and the behaviour of the animals was then recorded for 5 minutes. In our setup, no significant reaction to blue light was evident after an illumination with 3×10^{11} photons cm^{-2} s^{-1} and avoidance behaviour first occurred at 6×10^{11} photons cm^{-2} s^{-1} (Fig. 5C). Hence, to evaluate reactions to wavelengths outside the sensitivity maximum, the stimulus was delivered at twice the intensity of this value (i.e., 12×10^{11} photons cm^{-2} s^{-1}) in subsequent experiments.

To determine whether or not a shorter exposure to light would affect the significance of our results, we compared the animal's reaction to a 5, 3, 2, and 1 minute long illumination, respectively (supplementary material Fig. S3). The data show that illumination for 1 minute is sufficient to elicit a highly significant avoidance reaction. However, since about one third of all our animals did not respond to the 1-minute stimulus, we selected an illumination duration of 2 min for the remaining experiments (Fig. 5C).

For our major experiments, we again released groups of up to 6 animals (N=15 groups) in one half of the dark arena, which was then illuminated with quasi-monochromatic light of six different wavelengths of the same intensity (12×10^{11} photons cm^{-2} s^{-1}). In these experiments, *E. rowelli* specimens significantly evaded wavelengths ranging from UV to green light ($p<0.001$; Friedman-test with Dunn's post-test) but showed no evasive reaction to light of longer wavelengths ($p_{591}=0.343$, $p_{631}=0.650$; Friedman-test with Dunn's post-test) (Fig. 6A). In a final set of experiments, we tested our specimens for potentially positive phototaxis, as it is unknown whether or not they show preference for a particular wavelength. For these experiments, we used the same setting and released the animals in one half of the dark arena, but illuminated the other half with light of each of the six wavelengths, respectively. The obtained data gave no indication that the animals exhibit positive phototactic behaviour (Fig 6B; Friedman-test with Dunn's post-test: p_{465} and $p_{591}=0.769$, $p_{rest}>0.999$).

DISCUSSION

Onychophorans avoid wavelengths ranging from UV to green light

Our behavioural data provide evidence for negative phototaxis in the peripatopsid *E. rowelli*, corresponding to previous results from the peripatid *P. hitoyensis* (see Hering et al., 2012). In our tests, specimens of *E. rowelli* were not attracted by light but instead significantly avoided illumination with wavelengths ranging from UV to green light. The animals are unlikely to have reacted to heat rather than light, as there was no detectable increase of temperature in the arena even after illumination at maximum light intensity. The observed photonegative reaction is consistent with the nocturnal lifestyle and high susceptibility of onychophorans to desiccation (e.g. Manton and Ramsay, 1937; Bursell and Ewer, 1950; Eakin and Westfall, 1965; Read and Hughes, 1987). This might be one of the reasons why these animals generally avoid light, as it is a potential indicator of heat and low humidity.

The slow response of the onychophoran photoreceptors, as evidenced by a long time to peak and broad half width of the ERG signal in both species studied, is common in nocturnal invertebrates, which typically show slower reactions to light as compared to diurnal animals. This is regarded as an adaptation to dim light conditions, as the long latency and response duration generally enhance the sensitivity of visual organs (reviewed by Warrant, 2008; Fain et al., 2010; Warrant and Dacke, 2011). According to our behavioural sensitivity tests, the threshold for negative phototaxis in *E. rowelli* lies at 6×10^{11} photons cm^{-2} s^{-1} for blue light. This value corresponds well to light intensities typically found on the ground of rainforests during the day (e.g. Vazquez-Yanes et al., 1990), which, again, is in line with the nocturnal lifestyle of velvet worms that usually forage for food at night and seek shelter during the day (Read and Hughes, 1987; Mesibov, 1998).

Previous behavioural data from the peripatid *P. hitoyensis* indicated that the maximum sensitivity in this species lies within the blue-green range of the light spectrum (Hering et al., 2012). Our results based on ERGs from the eyes of *P. hitoyensis* and *E. rowelli* now provide more precise values, and the estimated maxima at $\lambda_{max} = 474 \pm 6.5$ nm in *E. rowelli* and $\lambda_{max} = 484$ nm in *P. hitoyensis* suggest that the eyes of both species are most sensitive to blue light, i.e. close to the lower limit of the previously estimated range (cf. fig. 4 in Hering et al., 2012). A maximum sensitivity to blue light is widespread among invertebrates with monochromatic vision, which might

be due to the maximum distribution of energy of solar radiation at about 480 nm (Menzel, 1979; Bowmaker and Hunt, 1999; Kelber and Roth, 2006).

Onychophorans exhibit monochromatic vision with onychopsin as the only visual pigment

The electrophysiologically determined spectral sensitivity of the dark-adapted eye could be well approximated assuming the presence of only one opsin-based visual pigment. Selectively adapting the retina to green light did not provide evidence for additional visual pigments maximally sensitive to shorter wavelengths. This finding is in line with the previous hypothesis of monochromatic vision in Onychophora, which is most likely based on an r-type opsin, the so-called onychopsin (Hering et al., 2012). However, since Eriksson et al. (2013) also detected a c-type opsin in the eye of *E. kanangrensis*, it was still debatable whether a c- or rather an r-type opsin is involved in onychophoran vision. Our *in situ* hybridization experiments in specimens of *E. rowelli* revealed *onychopsin* mRNA exclusively in the photoreceptor cell layer of the eye, but no expression in the brain (contrary to the claim of Eriksson et al., 2013) or other tissues. Conversely, we did not detect *Er-c-opsin* mRNA in the photoreceptor cells but rather in optic ganglion cells in the proximal portion of the eye as well as within the brain. In the brain, the majority of *Er-c-opsin*-positive somata occur in the ventromedian portion of the protocerebrum, but a few cell bodies are also found within the deutocerebrum. These findings, in particular the lack of *Er-c-opsin* expression in the photoreceptor cells, speak against an involvement of the c-opsin in onychophoran vision. We therefore conclude that onychopsin is most likely the only visual pigment in the onychophoran eye.

Although the function of the onychophoran c-opsin protein is unknown, it might be involved in non-visual, extra-ocular photoreception associated with circadian clock mechanisms (Fukada and Okano, 2002; Vigh et al., 2002; Arendt et al., 2004; Velarde et al., 2005; Shichida and Matsuyama, 2009). Notably, our expression data further indicate that the *Er-c-opsin* gene might be transcribed from both the sense and the antisense DNA strands, as our *in situ* hybridization experiments using the sense probe revealed a similar expression pattern of this gene to that using the antisense probe. The putative role of the *Er-c-opsin* antisense transcript in *E. rowelli* is unknown, but it might be involved in a self-regulation of the *Er-c-opsin* expression – a function that has been

suggested for other genes exhibiting antisense transcription (reviewed by Pelechano and Steinmetz, 2013).

Conclusions

Our electrophysiological data revealed maximum sensitivity to wavelengths around 480 nm in representatives of both major onychophoran subgroups, which suggests that the spectral absorption characteristics of the onychophoran photoreceptors in the retina have remained nearly unchanged for ~350 million years, i.e., since the divergence of Peripatidae and Peripatopsidae (Murienne et al., 2014). This might be due to the generally conserved geographic distribution and lifestyle of onychophorans, which are confined to humid habitats and exhibit cryptic, nocturnal behaviour (Manton and Ramsay, 1937; Bursell and Ewer, 1950; Read and Hughes, 1987; Mesibov, 1998; Oliveira et al., 2012). In conclusion, our electrophysiological recordings, behavioural experiments, and gene expression studies suggest that the onychophoran eye contains only one visual pigment, the r-type opsin onychopsin, which is most sensitive to blue light. The c-opsin is restricted to the brain, and may function in extra-ocular photoreception. Our data thus support the hypothesis of monochromatic vision in the last common ancestor of Panarthropoda (Hering et al., 2012; Hering and Mayer, 2014).

MATERIALS AND METHODS

Animals

Two species from the two major onychophoran subgroups were studied (Fig. 1A,B): *Principapillatus hitoyensis* Oliveira et al., 2012 (Peripatidae), and *Euperipatoides rowelli* Reid, 1996 (Peripatopsidae). Specimens of *P. hitoyensis* were collected from leaf litter in the Reserva Biológica Hitoy Cerere (Province of Limón, Region of Talamanca, Costa Rica; 09°40’N, 83°02’W, 300 m). Specimens of *E. rowelli* were obtained from decaying logs in the Tallaganda State Forest (New South Wales, Australia; 35°26’S, 149°33’E, 954 m). Onychophorans were collected and exported under the following permits: (1) the Forestry Commission of New South Wales, Australia (permit no. SL100159); and (2) the Gerencia Manejo y Uso Sostenible de RR NN–Ministerio del Ambiente y Energia, Costa Rica (permit numbers 123-2005-SINAC and 014950). The animals were kept in plastic boxes with perforated lids as described

267 previously (Baer and Mayer, 2012). Specimens of *P. hitoyensis* were maintained at
268 room temperature (20–24 °C), whereas those of *E. rowelli* were kept at 18 °C either in
269 the dark (for behavioural experiments), in the dark and under day/night conditions (for
270 gene expression studies), or under a shifted 14/10 hours day/night cycle and tested in
271 their active night period (in electrophysiological experiments). Behavioural experiments
272 were carried out at a normal day/night rhythm between 4 and 9 pm at 19 °C. All animal
273 treatments complied with the Principles of Laboratory Animal Care and the German
274 Law on the Protection of Animals.
275
276 **Electroretinograms**
277 To obtain ERGs, we fixed the anterior body portion of each analysed specimen to a
278 halved, tapered pipette tip (Fig. 2A) using dental silicone (polyvinyl siloxane,
279 PRESIDENT light body, Iso 4823; Coltène, Altstätten, Switzerland) or a combination
280 of dental silicone and a 1:1 mixture of beeswax and resin, taking care to leave one eye
281 and its surroundings free. In most cases, it was necessary to immobilise the animal
282 temporarily prior to handling by a 2–3 seconds long pulse of carbon dioxide from a soda
283 maker (Genesis, SodaStream®, Tel Aviv, Israel). The reference electrode, a chlorinated
284 silver wire, was brought in contact with the trunk of the specimen by conducting
285 electrode paste (Gel101, Biopac Systems Inc., Goleta, California, USA) and kept in
286 place with paper tissue wrapped around the trunk and the pipette tip. To prevent
287 dehydration, the tissue was soaked in saline based upon the composition of
288 onychophoran haemolymph (Robson et al., 1966). Just posterior or dorsal to the
289 exposed eye, the skin was thinned conically with the sharp tip of a broken razor blade.
290 This allowed us to penetrate the integument with an electrolytically sharpened tungsten
291 electrode for recording from the retina, while the skin closed tightly around the
292 electrode and resealed the puncture (Fig. 2B).
293 A white light stimulus was produced by a 200 W Xenon lamp (Cermax LX175F
294 ASB-XE-175EX, SP Spectral Products, Putnam, Connecticut, USA) and directed to the
295 eye via the central, 400 µm-wide fibre of a forked light guide (QR400-7-SR/BX, Ocean
296 Optics, Dunedin, Florida, USA), when two shutters (VS25S2ZM1R1 and LS6ZM2,
297 both Uniblitz, Vincent Associates®, Rochester, New York, USA) were opened. The
298 angular position and distance of the tip of the light guide to the eye were adjusted on a

goniometer such that the entire cornea was illuminated by the light beam of 16° divergence and ERG responses were maximized. Narrow-band interference filters (10–12 nm full width at half maximum; Melles Griot, Rochester, New York, USA) and neutral density filters (fused silica; also Melles Griot) could be inserted into the light path, providing spectral stimuli with equal photon flux from ultraviolet (330 nm) to red (700 nm) in 10 or 20 nm steps. All stimuli were delivered as flashes of 40 or 100 ms duration, separated by pauses of 3 or 5 s.

For spectral adaptation, light of a green light-emitting diode (LED) with a dominant wavelength of 521 nm and 34 nm full width at half maximum (LXHL-MM1D Green Luxeon Star, Quadica Developments Inc., Brantford, Ontario, Canada) was presented constantly throughout the experiment via the six outer fibres (each 400 μm in diameter) of the forked light guide. The combined light beam of 25° divergence provided between 3×10^{13} and 2×10^{16} photons cm^{-2} s^{-1} at the position of the eye, depending on the operating current of the LED and the distance between the cornea and the tip of the light guide.

Responses were amplified by a P15 AC amplifier (Natus Neurology Incorporated – Grass Technologies, Warwick, Rhode Island, USA) and sampled at 2000 Hz, digitized and saved using an NI PCIe-6251 data acquisition board and custom-made LabView scripts (both National Instruments Corporation, Austin, Texas, USA) installed on a conventional computer.

All experiments were carried out in a darkened Faraday cage with either the stimulus or the stimulus and the spectral adaptation light as the only light source. Adaptation periods prior to recording had to be kept to a minimum (2 to 5 minutes for spectral adaptation and 5 to 10 minutes for dark adaptation) due to the reduced viability of the animals in the setup. The spectral sensitivity under dark adaptation was measured up to 10 times, alternating between series starting with short and proceeding to long wavelengths, and series in the reverse order. Before and after each spectral series, a response-intensity (V-log I) relationship was determined to control for changes in recording quality and to establish the saturation level of responses. Initially, V-log I curves were measured with white light. When the peak sensitivity of an individual became evident, we used the available narrow-band spectral light closest to the presumed wavelength of maximal sensitivity for the V-log I. Up to three stable series in

both directions, i.e. six series altogether, were selected per individual and analysed using custom-made scripts in Matlab (R2012b, The MathWorks, Natick, Massachusetts, USA) as described in detail elsewhere (Telles et al., 2014). In short, the ERG was smoothed by a moving average with a window width of 0.01 s. Response amplitudes were calculated as potential changes from the baseline at stimulus onset to maximal hyperpolarization and converted into sensitivities based on the sigmoidal V-log I relationship obtained before and after each spectral series. We normalized all values to the maximal spectral sensitivity within a series and averaged series from the same individual. An established template for the absorbance of an opsin-based visual pigment (Govardovkii et al., 2000) was fitted to the entire mean spectral sensitivity curve using a non-linear least squares approach. We varied the amplitude and wavelength of the α peak and the amplitude of the β peak independently. Since the sensitivity curve for wavelengths below 390 nm was too flat to determine the wavelength of the β peak, we calculated it as a function of the α peak as suggested elsewhere (Govardovskii et al. 2000). Finally, the wavelengths of the estimated α peak (λ_{max}) and the respective coefficients of determination (R^2) were averaged for different individuals.

Fluorescence *in situ* hybridization

Partial sequences spanning most of the transmembrane region of the onychophoran r-type opsin (*Er-onychopsin*, 736 nt [CDS position 497–1232 of GenBank accession JN661372]) as well as the c-type opsin (*Er-c-opsin*, 808 nt [KM189804]) were amplified from cDNA, which was obtained by reverse transcription of total RNA (TRIzol® extraction protocol) using Superscript II and DNA Pol I polymerase (Invitrogen, Carlsbad, CA, USA) according to the manufacturer's protocols. The fragments were cloned using the pGEM®-T Vector System (Promega, Madison, WI, USA) and verified by Sanger sequencing (GATC Biotech, Konstanz, Germany). The cDNA clones were amplified by a standard M13 PCR and used directly to transcribe antisense and sense digoxigenin (DIG) labelled RNA probes by using SP6 and T7 RNA Polymerase, respectively, and the DIG RNA labelling mix (Roche Diagnostics, Rotkreuz, Switzerland). Freshly dissected heads of male specimens of *Euperipatoides rowelli* (N=10) were embedded and immediately frozen in Tissue-Tek® O.C.T.™ Compound (Sakura Finetek, Europe B.V.) and 10–16 µm thick horizontal sections were

cut on a Cryostat CM3050 S (Leica Biosystems, Nussloch, Germany). The sections were mounted on SuperFrost® plus slides (Menzel GmbH, Braunschweig, Germany), dried for 30 minutes at room temperature, and fixed in 4% paraformaldehyde for another 30 minutes. After several washing steps with PBST (PBS with 0.1% Tween® 20) and acetylation, the sections were pre-hybridized in hybridization buffer for 3–4 hours either at 55 °C or 58 °C and then hybridized for 12–16 hours at the same temperature using ~1 ng/µl RNA probe. Hybridization was followed by multiple washing steps with saline-sodium citrate buffer (SSC with 0.1% Tween® 20). The sections were incubated for 40 minutes in TNT buffer (0.1 M TRIS-HCl, pH 7.5; 0.15 M NaCl; 0.1% Tween® 20) containing 0.5% blocking reagent (PerkinElmer, Waltham, MA, USA). Anti-DIG-POD Fab-fragments (Roche Diagnostics), diluted either 1:50 or 1:100 in blocking solution, were then applied to the sections, which were incubated for additional 40–60 minutes at room temperature. After several washing steps with TNT buffer, the sections were incubated for 15 minutes with fluorescein-labelled tyramide (1:50 diluted working solution of the TSA™ Plus Fluorescein Fluorescence System; PerkinElmer). After counterstaining with propidium iodide for 15 minutes, the slides were mounted in Vectashield® mounting medium (Vector Laboratories, Burlingame, CA, USA) and analysed with a confocal laser-scanning microscope (Leica TCS STED; Leica Microsystems). Confocal image stacks were processed with LAS AF Lite v2.4.1 (Leica Microsystems).

Behavioural experiments

The initial light avoidance experiments to test for negative phototaxis were performed with single specimens of *E. rowelli* (N=12) as described previously for spectral experiments on *P. hitoyensis* (see Hering et al., 2012), except that only bright white light was presented. Each animal freely moved in a circular arena and its path was recorded 5 cm before and after stimulus presentation using the freely available video analysis and modelling tool Tracker (Douglas Brown, http://www.cabrillo.edu/~dbrown/; v.4.05 [09/04//2013]). The paths of the animals tested were then plotted into a single diagram (Fig. 5A,B). The statistical analysis was conducted by comparing the turning angles of the animals under illumination to the

control runs without the stimulus by applying the Wilcoxon signed rank test (see Hering et al., 2012).

The remaining behavioural experiments were performed with a modified version of the setup introduced by Monge-Nájera et al. (1993) using a rectangular arena (163×93×70 mm) made of acrylic glass enclosed in black paper (Fig. 2C). A grey opaque, removable plastic plate separated the arena in two halves. One half could be illuminated by a cold light source via a double-ended light guide (Fig. 2C,D). For each experiment, the bottom of the arena was covered with a sheet of the same white paper towels that were used for maintaining the animals (Baer and Mayer, 2012). The sheet was folded three times, cut to the size of the arena and wetted with 5 ml distilled water, thus ensuring equal humidity in all experiments. No space was left between the paper towel and the border of the arena to prevent the animals from escaping under the paper towel.

All experiments were carried out in total darkness at 19.3 ± 0.6 °C. The light stimulus was delivered by narrow-banded LEDs (Nichia Corporation, Tokushima, Japan and Avago Technologies, San José, CA, USA). The LEDs emitted no light in the infrared range, and thus generated no detectable heat. To control for the possibility of the animals' reaction to heat rather than light, the temperature at the bottom of the arena was measured after illumination for 5 minutes with each LED at maximum intensity (i.e. for the 373, 402, 465, 528, 591 and 631 nm LEDs, the maximum intensity was 40, 220, 370, 130, 90 and 160 times higher than that used in our behavioural experiments, respectively). These measurements revealed no stimulus-correlated change in temperature. The stimulus was generated by the PowerLab 26T data acquisition system (AD Instruments, Dunedin, New Zealand) and equalised by using different output voltages and neutral density filters (Tinxi GmbH, Eggenstein-Leopoldshafen, Germany). On- and offset of the stimulus was triggered with the Chart software (v5.5.6; AD Instruments). An infrared-sensitive camera (Sony Handycam HDR-HC7, Tokyo, Japan) was mounted above the arena to automatically record the experiments. To avoid potential bias caused by possible physical or chemical influence, such as smell, noise, heat, or mechanical vibrations, all scoring and analyses were computerised and performed with the experimenter distant from the recording arena, except when releasing the animals. Before the next trial, the entire arena was cleaned and the paper

towels renewed to remove any traces left by the animals. In addition, the entire setup was rotated by 90° every second day.

To determine the optimal duration and illumination intensity for the main behavioural experiments, 7 groups of up to 6 specimens of *E. rowelli* (34 individuals in total) were dark-adapted for 20 minutes and placed in the illuminable half of the arena. After leaving them to settle for two minutes, the plastic plate separating the two halves was removed, the light switched on and each group tested for four different intensities (3×10^{11}, 6×10^{11}, 9×10^{11}, 12×10^{11} photons cm^{-2} s^{-1}) of the 465 nm blue light. The movements of the animals were recorded for 1, 2, 3 or 5 minutes (supplementary material Fig. S3).

These experiments revealed the optimal duration (2 minutes) and illumination intensity (twice the identified threshold, i.e. 12×10^{11} photons cm^{-2} s^{-1}), which were then used for the major behavioural experiments. For these experiments, narrow-band lights of six different wavelengths were used: 373 ± 13 nm, 402 nm ± 10 nm, 465 nm ± 19 nm, 528 nm ± 26 nm, 591 nm ± 14 nm, and 631 nm ± 21 nm total width at half-maximum, respectively (Fig. 2E). Like in the preliminary tests, up to six specimens were grouped (N=15 groups, 80 animals in total), dark-adapted for 20 minutes and tested in parallel. Each group experienced one run per day. In the tests for negative phototaxis (N=15 groups in total, three trials per wavelength), the animals were placed in the illuminable half of the arena, whereas in those for positive phototaxis (N=15 groups in total, one trial per wavelength) they were set in the dark half of the arena. The behaviour of the animals was recorded for 2 minutes after the light was switched on. Experiments, in which animals interacted (e.g. pushed or bit each other, or aggregated), were not analysed, and the animals were retested the following day (30 out of 410 experiments, 7.3%). To exclude potential biases, the wavelength of the presented light stimulus was changed randomly every day, only precluding the use of the neighbouring wavelengths in subsequent tests.

In all experiments, the time each animal spent in the dark half of the arena was measured, averaged for all specimens of the group and divided by the total experimental time. This resulted in a value ranging from 0 for no avoidance to 1 for total avoidance. The obtained data were analysed using the non-parametric Friedman-test, followed by Dunn's multiple comparison test to compare each wavelength against the control runs.

These calculations were performed using the statistics program Prism v.6 (GraphPad Software, La Jolla, CA, USA) and plotted with Adobe Illustrator CS5.1 (Adobe Systems, San José, CA, USA).

Acknowledgements

We are thankful to Noel Tait, David Rowell, Ivo de Sena Oliveira, Franziska Anni Franke, Michael Gerth, and Sandra Treffkorn for help with specimen collection, to Ivo de Sena Oliveira for help with macrophotography, to Christine Martin for assistance with confocal microscopy, to Johanna Chavez and Martin Kohler for conducting behavioural pilot experiments, to Kerstin Flieger, Matthias Gilbert and Lars Thomas for help with calibrating the behavioural setup, to Klaus Schildberger, Dan-Eric Nilsson, Eric Warrant and Thomas Labhart for providing access to various equipment, to Ronald Petie for assistance in constructing the ERG setup, to David O'Carroll for valuable advice on the electrophysiological recording technique, and to Uwe Mayer for helpful comments on the first draft of the manuscript. The staffs of the Forestry Commission of New South Wales (NSW, Australia), the Instituto Nacional de Biodiversidad (INBio, Costa Rica), and the National System of Conservation Areas (SINAC, MINAE, Costa Rica) are gratefully acknowledged for providing permits.

Competing interests

The authors declare no competing interests.

Author contributions

H.B., P.A.S. and G.M. designed the behavioural experiments and H.B. carried out these experiments and analysed the data. M.H. and A.K. designed the electrophysiological experiments and H.B. and M.H. performed these experiments and analysed the data. L.H. and G.M. designed the gene expression experiments and L.H. carried out these experiments. G.M. and P.A.S. provided the setup and analysing tools for the behavioural experiments and A.K. contributed the electrophysiology setup. H.B. wrote the first draft and all authors read, made comments on and approved the final manuscript.

Funding

This work was supported by grants from the Studienstiftung des deutschen Volkes [German National Merit Foundation; 186861 to H.B.]; the Emmy Noether Programme of the German Research Foundation [Ma 4147/3-1 to G.M.]; and the K. & A. Wallenberg-Foundation and the Swedish Research Council [2012–2212 to A.K.].

Supplementary material

Supplementary material available online at

http://jeb.biologists.org/lookup/suppl/doi:XXX

REFERENCES

Arendt, D., Tessmar-Raible, K., Snyman, H., Dorresteijn, A. W. and Wittbrodt, J. (2004). Ciliary photoreceptors with a vertebrate-type opsin in an invertebrate brain. *Science* **306**, 869–871.

Baer, A. and Mayer, G. (2012). Comparative anatomy of slime glands in Onychophora (velvet worms). *J. Morphol.* **273**, 1079–1088.

Bowmaker, J. K. and Hunt, D. M. (1999). Molecular biology of photoreceptor spectral sensitivity. In *Adaptive Mechanisms in the Ecology of Vision*, eds. S. N. Archer M. B. A. Djamgoz E. R. Loew J. C. Partridge and S. Vallerga), pp. 439–462: Springer Netherlands.

Briscoe, A. D. and Chittka, L. (2001). The evolution of color vision in insects. *Annu. Rev. Entomol.* **46**, 471–510.

Bursell, E. and Ewer, D. W. (1950). On the reactions to humidity of *Peripatopsis moseleyi* (Wood-Mason). *J. Exp. Biol.* **26**, 335–353.

Eakin, R. M. and Westfall, J. A. (1965). Fine structure of the eye of peripatus (Onychophora). *Z. Zellforsch. Mikrosk. Anat.* **68**, 278–300.

Eriksson, B. J., Fredman, D., Steiner, G. and Schmid, A. (2013). Characterisation and localisation of the opsin protein repertoire in the brain and retinas of a spider and an onychophoran. *BMC Evol. Biol.* **13**, 186.

Fain, G. L., Hardie, R. and Laughlin, S. B. (2010). Phototransduction and the evolution of photoreceptors. *Curr. Biol.* **20**, R114–124.

Fukada, Y. and Okano, T. (2002). Circadian clock system in the pineal gland. *Mol. Neurobiol.* **25**, 19–30.

Giribet, G. and Edgecombe, G. D. (2012). Reevaluating the arthropod tree of life. *Annu. Rev. Entomol.* **57**, 167–186.

Govardovkii, V. I., Fyhrquist, N., Reuter, T., Kuzmin, D. G. and Donner, K. (2000). In search of the visual pigment template. *Vis. Neurosci.* **17**, 509–528.

Hering, L. and Mayer, G. (2014). Analysis of the opsin repertoire in the tardigrade *Hypsibius dujardini* provides insights into the evolution of opsin genes in Panarthropoda. *Genome Biol. Evol.* **6**, 2380–2391.

Hering, L., Henze, M. J., Kohler, M., Kelber, A., Bleidorn, C., Leschke, M., Nickel, B., Meyer, M., Kircher, M., Sunnucks, P. et al. (2012). Opsins in Onychophora (velvet worms) suggest a single origin and subsequent diversification of visual pigments in arthropods. *Mol. Biol. Evol.* **29**, 3451–3458.

Kelber, A. and Roth, L. S. (2006). Nocturnal colour vision – not as rare as we might think. *J. Exp. Biol.* **209**, 781–788.

Manton, S. M. and Ramsay, J. A. (1937). Studies on the Onychophora. III. The control of water loss in *Peripatopsis J. Exp. Biol.* **14**, 470–472.

Mayer, G. (2006). Structure and development of onychophoran eyes: What is the ancestral visual organ in arthropods? *Arthropod. Struct. Dev.* **35**, 231–245.

Menzel, R. (1979). Spectral Sensitivity and Color Vision in Invertebrates. In *Comparative Physiology and Evolution of Vision in Invertebrates*, vol. 7 / 6 / 6 A (ed. H. Autrum), pp. 503–580: Springer Berlin Heidelberg.

Mesibov, B. (1998). Curious, yes, but not all that rare. *Invertebrata* **11**, 6.

Monge-Nájera, J., Barrientos, Z. and Aguilar, F. (1993). Behavior of *Epiperipatus biolleyi* (Onychophora: Peripatidae) under laboratory conditions. *Rev. Biol. Trop.* **41**, 689–696.

Murienne, J., Daniels, S. R., Buckley, T. R., Mayer, G. and Giribet, G. (2014). A living fossil tale of Pangean biogeography. *Proc. R. Soc. B.* **281**, 1471–2954.
Oliveira, I. S., Read, V. M. S. J. and Mayer, G. (2012). A world checklist of Onychophora (velvet worms), with notes on nomenclature and status of names. *ZooKeys* **211**, 1–70.
Pelechano, V. and Steinmetz, L. M. (2013). Gene regulation by antisense transcription. *Nat. Rev. Genet.* **14**, 880–893.
Porter, M. L., Blasic, J. R., Bok, M. J., Cameron, E. G., Pringle, T., Cronin, T. W. and Robinson, P. R. (2012). Shedding new light on opsin evolution. *Proc. R. Soc. B.* **279**, 3–14.
Read, V. M. S. J. and Hughes, R. N. (1987). Feeding behaviour and prey choice in *Macroperipatus torquatus* (Onychophora). *Proc. R. Soc. B.* **230**, 483–506.
Robson, E. A., Lockwood, A. P. M. and Ralph, R. (1966). Composition of the blood in Onychophora. *Nature* **209**, 533.
Shichida, Y. and Matsuyama, T. (2009). Evolution of opsins and phototransduction. *Philos. Trans. R. Soc. B Biol. Sci.* **364**, 2881–2895.
Stavenga, D. (2010). On visual pigment templates and the spectral shape of invertebrate rhodopsins and metarhodopsins. *J. Comp. Physiol. A.* **196**, 869–878.
Telles, F. J., Lind, O., Henze, M. J., Rodriguez-Girones, M. A., Goyret, J. and Kelber, A. (2014). Out of the blue: the spectral sensitivity of hummingbird hawkmoths. *J. Comp. Physiol. A.* **200**, 537–546.
Vazquez-Yanes, C., Orozco-Segovia, A., Rincón, E., Sánchez-Coronado, M. E., Huante, P., Toledo, J. R. and Barradas, V. L. (1990). Light Beneath the Litter in a Tropical Forest: Effect on Seed Germination. *Ecology* **71**, 1952–1958.
Velarde, R. A., Sauer, C. D., O. Walden, K. K., Fahrbach, S. E. and Robertson, H. M. (2005). Pteropsin: a vertebrate-like non-visual opsin expressed in the *honey bee* brain. *Insect Biochem. Mol. Biol.* **35**, 1367–1377.
Vigh, B., Manzano, M., Zádori, A., Frank, C., Lukáts, A., Röhlich, P., Szél, A. and Dávid, C. (2002). Nonvisual photoreceptors of the deep brain, pineal organs and retina. *Histol. Histopathol.* **17**, 555-590.
Warrant, E. (2008). Nocturnal Vision. In *The Senses: A Comprehensive Reference*, eds. R. H. Masland T. D. Albright P. Dallos D. Oertel S. Firestein G. K. Beauchamp M. C. Bushnell A. I. Basbaum J. H. Kaas and E. P. Gardner), pp. 53–86. New York: Academic Press.
Warrant, E. and Dacke, M. (2011). Vision and Visual Navigation in Nocturnal Insects. *Annu. Rev. Entomol.* **56**, 239–254.

584 **FIGURE LEGENDS**

585 **Fig. 1. Position of eyes in the two onychophoran species studied, *Euperipatoides***
586 ***rowelli* and *Principapillatus hitoyensis*.** Both species possess a pair of simple lateral
587 eyes, one at the base of each antenna (arrowheads). Scale bars: 500 µm. (A) The
588 peripatopsid *E. rowelli*. (B) The peripatid *P. hitoyensis*. Details in A and B are from
589 specimens preserved in 70% ethanol.

590

591 **Fig. 2. Experimental design of the electrophysiological and behavioural**
592 **experiments.** (A) Diagram of an electrophysiological preparation. The head of a
593 specimen is embedded in dental cement (green), so that only the area surrounding the
594 eye is accessible for the electrode and the light guide (light cone indicated in blue). (B)
595 Diagram of a sagittal section of the eye (based on a histological section from Mayer,
596 2006) illustrating the desired position of the electrode. Anterior is left. The electrode
597 does not penetrate the cornea of the eye but is inserted through the adjacent cuticle and
598 tissue. (C) Top view of the arena used for behavioural experiments. Only one half was
599 illuminated (indicated in light-blue). (D) Overview of the entire behavioural setup. (E)
600 Normalised emission spectra of the narrow-banded light-emitting diodes used in the
601 behavioural setup. Abbreviations: an, antenna; ar, arena; ca, video camera; co, cornea;
602 ct, connective tissue; da, dark half of the arena; dp, dermal papilla; el, electrode; ey, eye;
603 ia, illuminated half of the arena; le, leg; lg, light guide; og, optic ganglion cells; on,
604 optic neuropil; os, outer segments of photoreceptors; pl, perikaryal layer of
605 photoreceptors; sp, slime papilla; tr, trunk; vb, vitreous body (=lens-like structure).

606

607 **Fig. 3. Spectral sensitivity of the eye in the peripatopsid *E. rowelli* and the**
608 **peripatid *P. hitoyensis* determined by electroretinograms (ERGs).** (A,C) ERGs
609 recorded for flashes of white light with increasing intensity (upper trace) consisted of an
610 initial hyperpolarization truncated by a depolarization (lower trace). Response
611 amplitudes (insets) were calculated as potential changes from the baseline at stimulus
612 onset to maximal hyperpolarization. Dots represent measurements, for which no ERG is
613 shown. (B,D) Averaged spectral sensitivity of the eye in two individuals (mean ±
614 standard deviation, six measurements per data point) based on response amplitudes to
615 light stimuli of different wavelengths and equal photon flux. Fitting a template (grey

line) for the absorbance of an opsin-based visual pigment to the measurements yielded a wavelength of peak absorbance (λ_{max}) of about 480 nm with a coefficient of determination (R^2) over 0.9 for both species.

Fig. 4. Expression pattern of *Er-onychopsin* and *Er-c-opsin* mRNA in the peripatopsid *E. rowelli* visualised using antisense probes. Horizontal sections of heads. Anterior is up in all images. Light (A) and confocal micrographs (B–F) illustrating the results of fluorescence *in situ* hybridization experiments using antisense RNA probes which were visualized using fluorescein-labelled tyramide. DNA was stained using propidium iodide. (A) Cryosection showing the spatial relationship of the eyes to the brain (dashed line). Scale bar: 250 µm. (B) Section at the level of the eyes demonstrating the expression of *Er-onychopsin* in the eyes but not in the brain or other tissues. Scale bar: 250 µm. (C) Section of an eye showing that *Er-onychopsin* is expressed exclusively in the photoreceptor cell layer (arrows). The cuticle exhibits autofluorescence, which is also evident in sections labelled with the sense probe as a negative control (see supplementary material Fig. S2). Scale bar: 50 µm. (D) Detail of the photoreceptor cell layer. *Er-onychopsin* expression is restricted to the perikarya surrounding each nucleus (arrows). Scale bar: 10 µm. (E) Overview of *Er-c-opsin* expression in a section of the head at the level of the eyes. *Er-c-opsin* is expressed in the deutocerebrum (arrows) and in the optic ganglion cells (arrowhead) in the proximal portion of the eye (sectioned horizontally on the left side; see inset in the lower right corner for a higher magnification; scale bar: 10 µm). Note the lack of signal in the photoreceptor cell layer of the eye on the right side. Scale bar: 250 µm. (F) Overview of *Er-c-opsin* expression in a section through the ventral part of the brain at the level of the mushroom bodies. *Er-c-opsin* is expressed in the median portion of the protocerebrum (arrows) and in the connecting cords linking the brain to the ventral nerve cord (arrowheads). Scale bar: 250 µm. Inset in the lower left corner shows detail of expression in the medioventral perikaryal layer within the protocerebrum. Scale bar: 10 µm. Abbreviations: at, antennal tract; br, brain; cn, central brain neuropil; cc, connecting cord; co, cornea; de, deutocerebrum; dp, dermal papilla; ep, epidermis; ey, eye; fn, frontal brain neuropil; lu, lumen of the eye vesicle; mb, mushroom body; og,

optic ganglion cell layer; on, optic neuropil; pc, photoreceptor cell layer; pe, perikaryal layer of the brain; ph, pharynx; vb, vitreous body.

Fig. 5. Light avoidance behaviour in the peripatopsid *E. rowelli*. (A) White light: Plotted pathways of N=12 *E. rowelli* (Peripatopsidae), each tested twice (n= 24). Bright white light was presented onto the head of each animal. All animals change their walking direction and turn away from the light stimulus as compared to the control (B). The pathways of the same 12 animals are unaffected when no light was presented. The differences in turning are highly significant ($p<0.001$; Wilcoxon-signed-rank test). (C) Sensitivity threshold of *E. rowelli* under 5 and 2 minutes of blue light illumination (λ_{max} = 465 nm). Boxplots (N=7 groups of up to 6 animals, circles give the median, boxes the quartiles and whiskers represent 10/90 percentiles) illustrate the fraction of time spent in the dark half of the arena relative to the total time of the test. Significant avoidance reaction (** $p<0.01$; Friedman-test with Dunn's post-test) occurs at an intensity of 6×10^{11} photons cm^{-2} s^{-1}, whereas no significant reaction is seen at 3×10^{11} cm^{-2} s^{-1} (ns, $p=0.570$; Friedman-test with Dunn's post-test).

Fig. 6. Behavioural response to light stimuli of equal quanta of different wavelengths in the peripatopsid *E. rowelli*. Groups (N=15) of up to 6 animals were stimulated for 2 minutes with a spectral light stimulus of 12×10^{11} photons cm^{-2} s^{-1}. In control experiments, the LEDs remained switched off. Friedman-test with Dunn's post-test was used for data analysis. Boxplots (format as in Fig. 5) illustrating the fraction of time spent in the dark half of the arena relative to the total test time. Colours symbolise the wavelengths used. (A) Animals started in the illuminated half and showed negative phototactic behaviour to the light spectrum ranging from UV to green (*** $p<0.001$), but not to longer wavelengths ($p_{591}=0.343$ and $p_{631}=0.650$, ns=not significant). Every group is represented by a mean of three repetitions per wavelength. Dashed line indicates the average spectral sensitivity curve for *E. rowelli* obtained from electrophysiological recordings, with the baseline adjusted to the median of the behavioural control and the maximum standardised to 1. (B) Animals started in the dark half of the arena, while the other half was illuminated. No significant difference from

678 the control is evident for any of the tested wavelengths (p_{465} and p_{591}=0.769,
679 p_{others}>0.999). Dashed line indicates the median of the control.

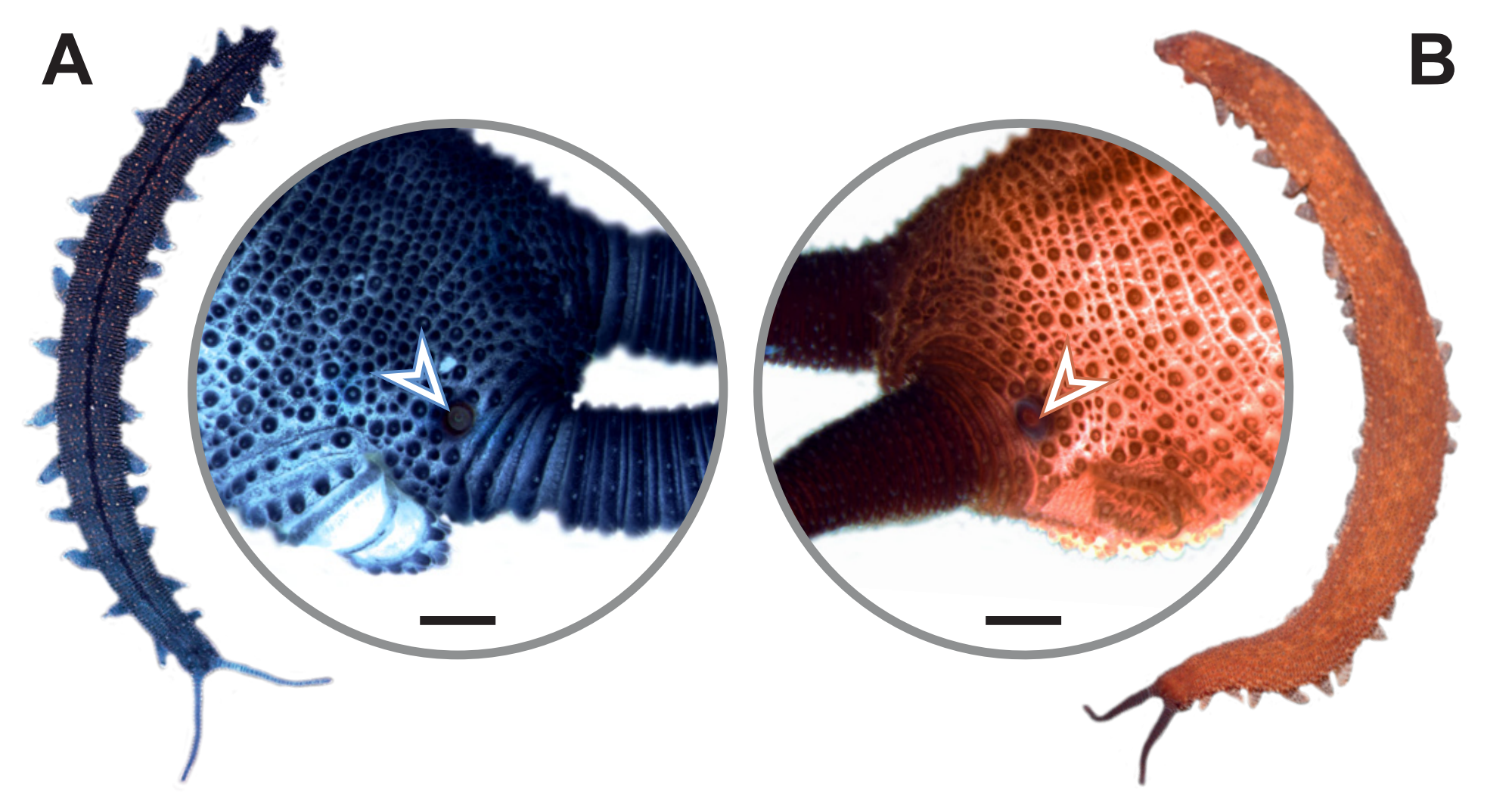
A
B

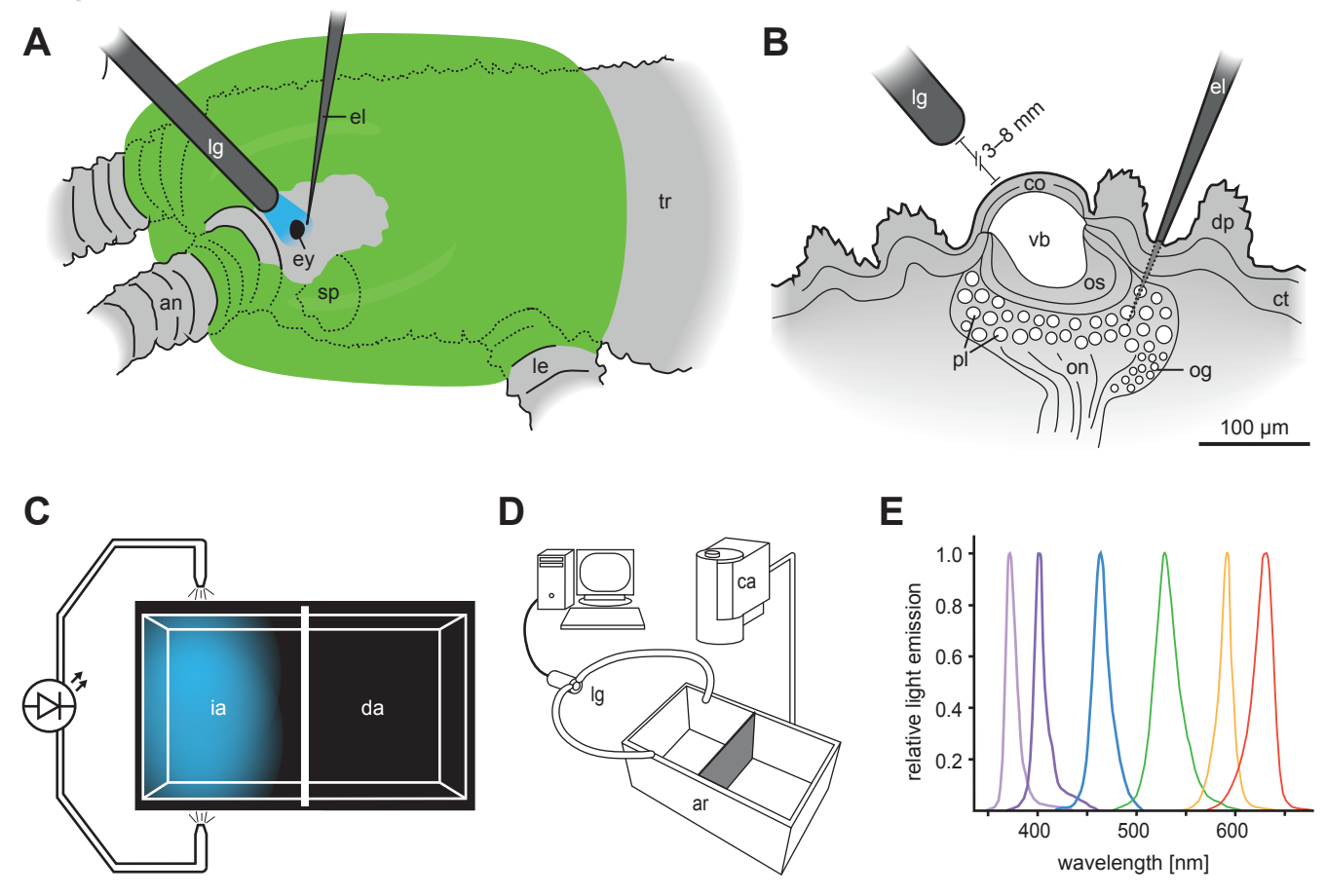
A
lg
el
ey
sp
an
tr
le
B
lg
3–8 mm
el
co
vb
os
dp
ct
pl
on
og
100 µm
C
ia
da
D
ca
lg
ar
E
relative light emission
1.0
0.8
0.6
0.4
0.2
400
500
600
wavelength [nm]

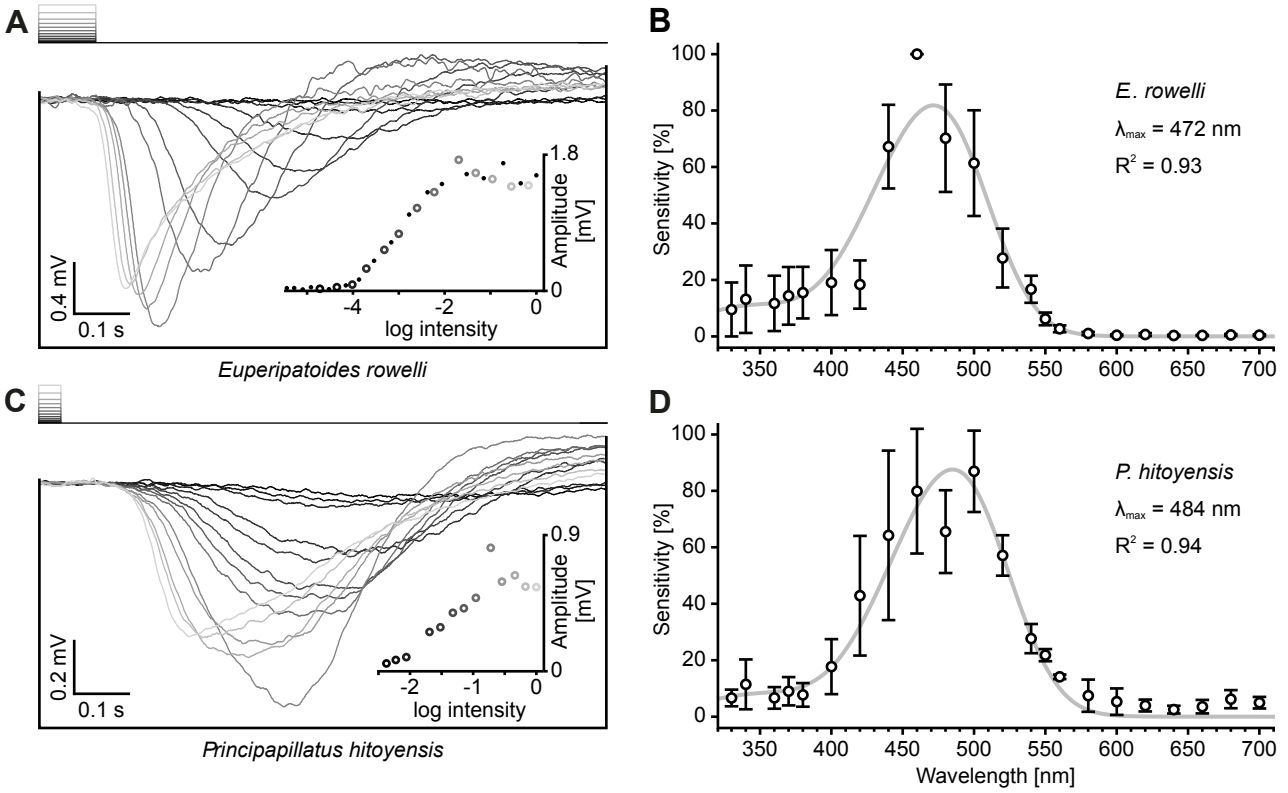
A
0.4 mV
0.1 s
1.8
Amplitude [mV]
0
-4
-2
0
log intensity
Euperipatoides rowelli
B
Sensitivity [%]
E. rowelli
λmax = 472 nm
R2 = 0.93
C
0.2 mV
0.1 s
0.9
Amplitude [mV]
0
-2
-1
0
log intensity
Principapillatus hitoyensis
D
Sensitivity [%]
P. hitoyensis
λmax = 484 nm
R2 = 0.94
Wavelength [nm]

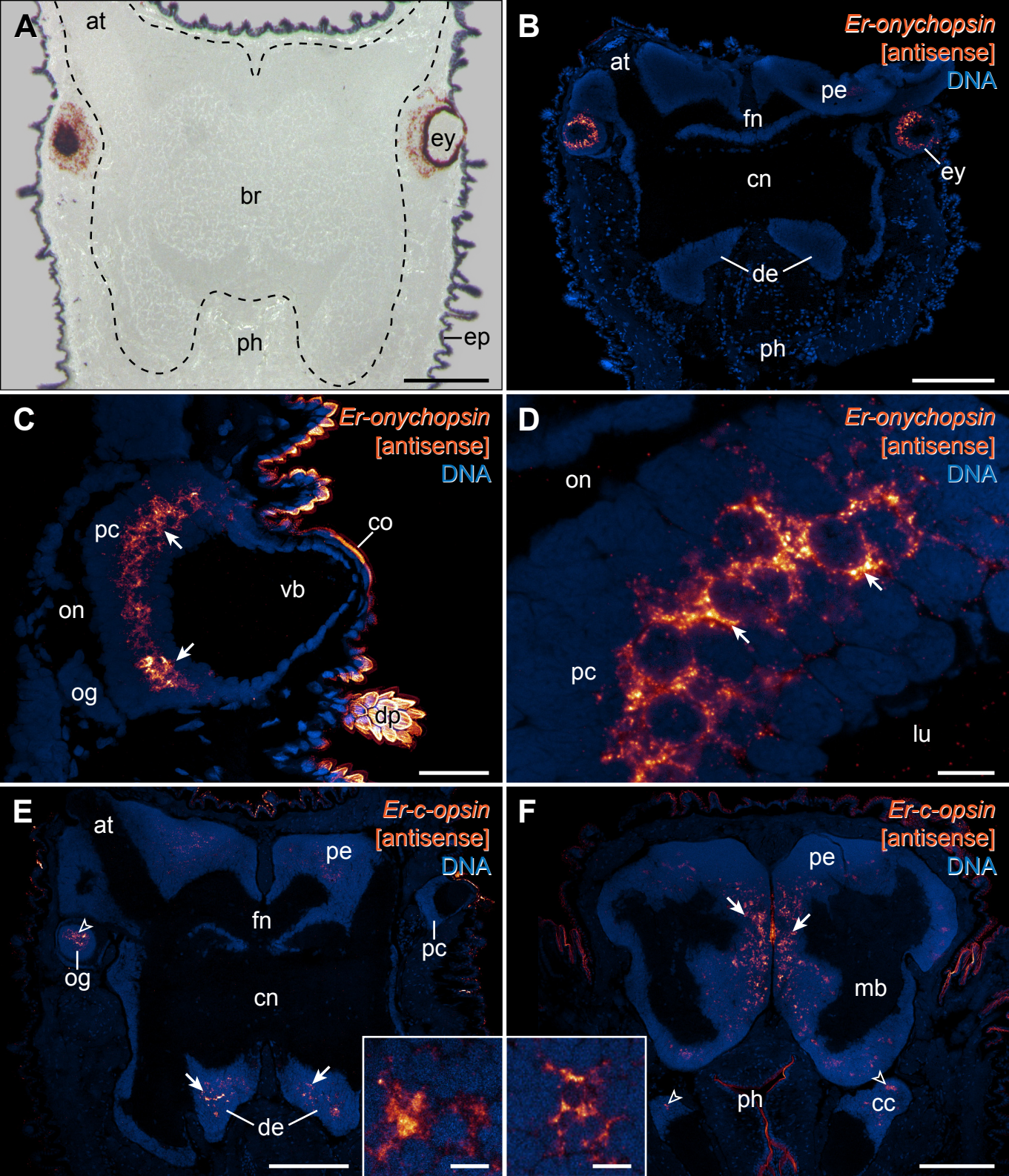
A
at
ey
br
ph
ep
B
Er-onychopsin
[antisense]
DNA
at
pe
fn
ey
cn
de
ph
C
Er-onychopsin
[antisense]
DNA
pc
co
vb
on
og
dp
D
Er-onychopsin
[antisense]
DNA
on
pc
lu
E
Er-c-opsin
[antisense]
DNA
at
pe
fn
pc
og
cn
de
F
Er-c-opsin
[antisense]
DNA
pe
mb
ph
cc

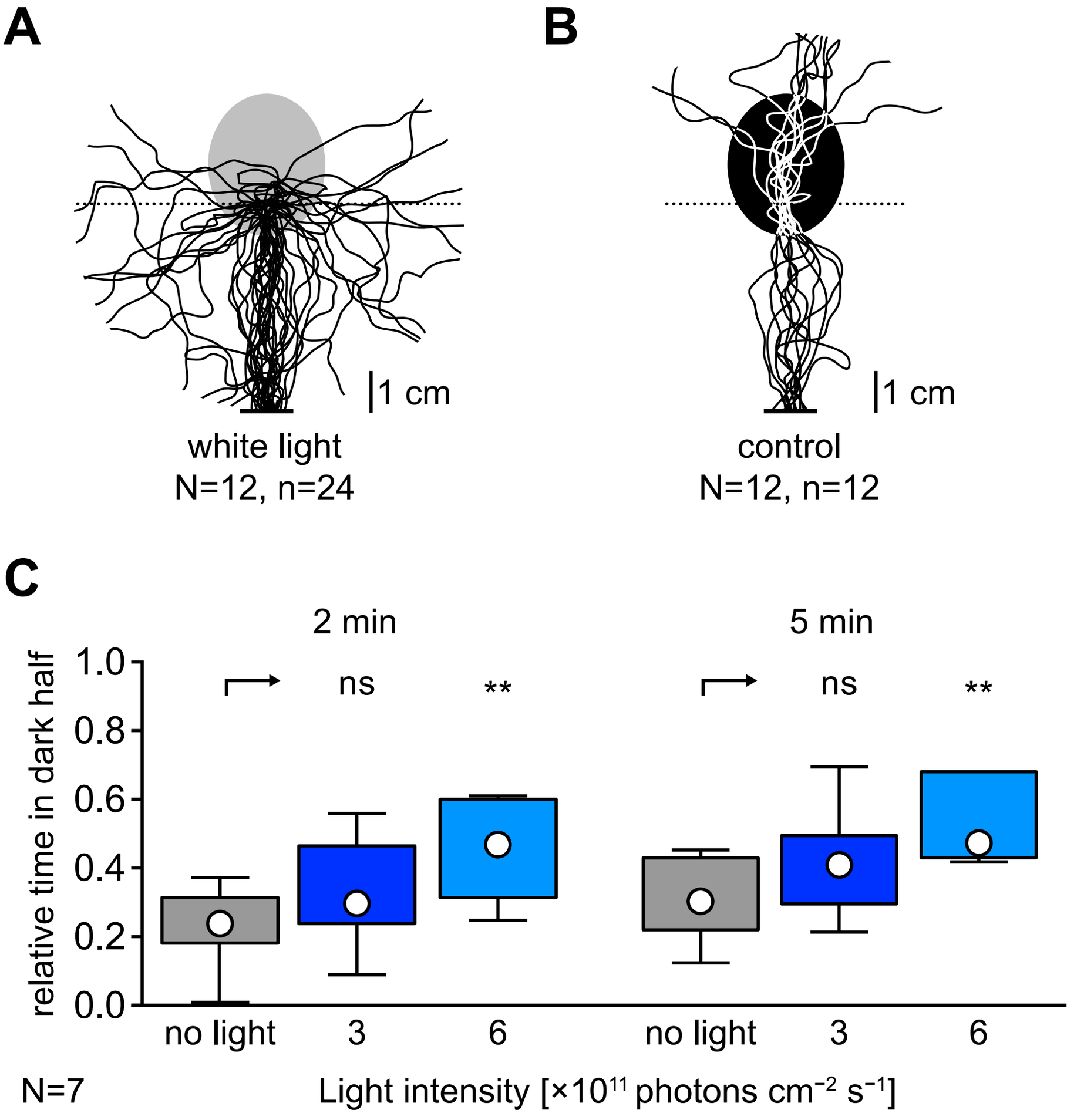
A
B
1 cm
1 cm
white light
N=12, n=24
control
N=12, n=12
C
2 min
5 min
ns
**
ns
**
relative time in dark half
1.0
0.8
0.6
0.4
0.2
0.0
no light
3
6
no light
3
6
N=7
Light intensity [×10^11 photons cm^−2 s^−1]

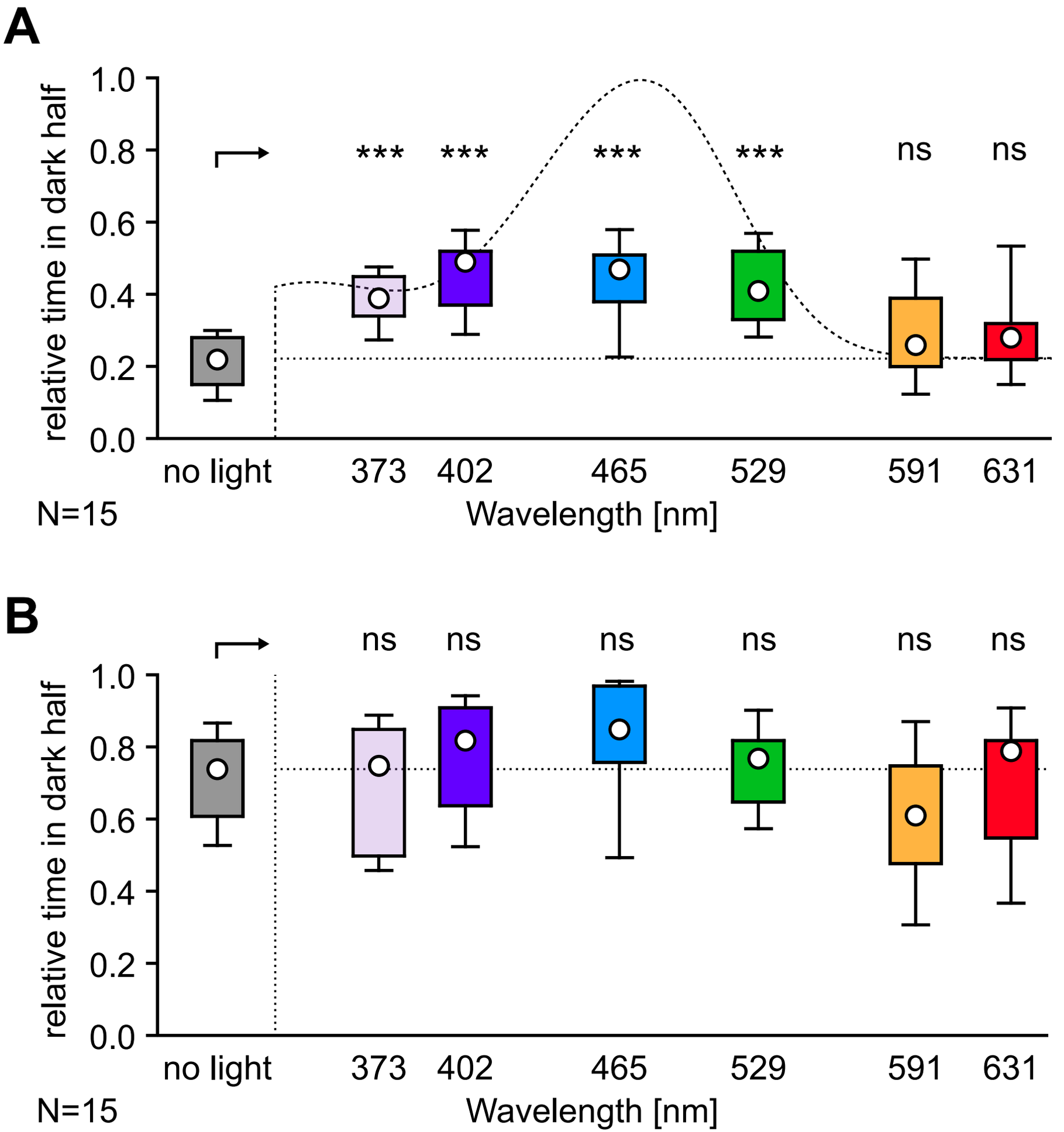
A
relative time in dark half
1.0
0.8
0.6
0.4
0.2
0.0
***
***
***
***
ns
ns
no light
373
402
465
529
591
631
N=15
Wavelength [nm]
B
relative time in dark half
1.0
0.8
0.6
0.4
0.2
0.0
ns
ns
ns
ns
ns
ns
no light
373
402
465
529
591
631
N=15
Wavelength [nm]